

esac

European Space Astronomy Centre (ESAC)
European Space Agency (ESA)
Camino Bajo del Castillo s/n
Urb. Villafranca del Castillo
28692 Villanueva de la Canada - Madrid
SPAIN

CASSIS CO-REGISTERED SUPER-RESOLUTION IMAGES AND MADNET-DERIVED DIGITAL TERRAIN MODELS OF OXIA PLANUM OF MARS

APPROVAL CHANGE LOG

Reason for change	Issue	Revision	Date
Initial version	1	0	14/12/2021

CHANGE RECORD

Issue 1	Revision 0		
Reason for change	Date	Pages	Paragraph(s)
Initial version	14/12/2021	All	All



TABLE OF CONTENTS:

1. Introduction.....	4
1.1 Instrument and Datasets.....	4
1.2 Abbreviations and Acronyms.....	6
1.3 Reference and Applicable Documents.....	7
2. Scientific Objectives.....	8
2.1 Acknowledgements.....	8
3. Data Product Generation.....	9
3.1 Product Overview.....	10
3.2 SRR and SRR-DTM Product Specification.....	12
3.3 Product Example and Usage.....	12
4. Known Issues.....	14
5. Software.....	16

1. INTRODUCTION

High-resolution digital terrain models (DTMs) and their corresponding terrain-corrected orthorectified images (ORIs) are probably two of the most fundamental and intuitive resources for studying the Martian surface. Apart from the globally available lower resolution (463 m/pixel) Mars Orbiter Laser Altimeter (MOLA) DTM, higher resolution Mars DTMs are typically produced from the 12.5 – 50 m/pixel Mars Express High Resolution Stereo Camera (HRSC) images, the 6 m/pixel Mars Reconnaissance Orbiter (MRO) Context Camera (CTX) images, the ~4.6 m/pixel (4 m/pixel nominal resolution) ExoMars Trace Gas Orbiter (TGO) Colour and Stereo Surface Imaging System (CaSSIS) images, and the ~30 cm/pixel (25 cm/pixel nominal resolution) MRO High Resolution Imaging Science Experiment (HiRISE) images. The DTM products derived from these imaging sources often have different effective resolutions and spatial coverage, depending on the properties of the input images and the DTM retrieval methods, which include traditional photogrammetric methods, photogrammetry methods, and deep learning-based methods.

It has been a common situation that DTMs derived from a particular imaging dataset can only achieve a lower, or at the best, similar effective spatial resolution compared to the input images, due to the various approximations and/or filtering processes introduced by the photogrammetric or photogrammetric pipelines. With recent successes in deep learning techniques, it has now become practical to improve the effective resolution of an image using super-resolution restoration (SRR) networks (*Tao et al., 2021a*), retrieving pixel-scale topography using single-image DTM estimation (SDE) networks (*Tao et al., 2021b*), and eventually, combining the two techniques to potentially produce subpixel-scale topography from only a single-view input image (*Tao et al., 2021c*).

In this work, we have combined the use of SRR and SDE to boost the effective resolution of optical single-image-based DTMs to subpixel-scale. The in-house implementations of the MARSCHAN (multi-scale adaptive-weighted residual super-resolution generative adversarial network) SRR system (*ibid*) and the MADNet (multi-scale generative adversarial U-net based single-image DTM estimation) SDE system (*ibid*) are employed for this work. The study site is within the 3-sigma ellipse of the Rosalind Franklin ExoMars rover's planned landing site (centred near 18.275°N, 335.368°E) at Oxia Planum. We use the 4 m/pixel TGO CaSSIS "PAN" band images as the input dataset. We apply MARSCHAN SRR to the original CaSSIS and HiRISE images, and subsequently, we apply MADNet SDE to the resultant 1 m/pixel CaSSIS SRR to produce CaSSIS SRR-DTMs at 2 m/pixel. Qualitative and quantitative assessments for the resultant CaSSIS SRR-DTMs are shown in (*Tao et al., 2021c*).

1.1 Instrument and Datasets

TGO CaSSIS is a moderately high-resolution, multispectral (from ~500 nm to ~950 nm for visible and near-infrared (NIR)), push-frame (an intermedium of a line scan camera and frame camera) stereo imager, with the goal of extending the coverage of the MRO HiRISE camera and to produce moderately high-resolution DTMs of the Martian surface. CaSSIS provides colour images consisting of the "BLU" band (centred at 499.9 nm for blue-green), the "PAN" band (centred at 675.0 nm for orange-red), the "RED" band (centred at 836.2 nm for NIR), and the "NIR" band (centred at 936.7 nm for NIR). CaSSIS images are typically sampled at 4 m/pixel nominal spatial resolution (~4.6 m/pixel effective spatial resolution) with a swath width of about 9.5 km and a swath length of about 30 – 40 km. Due to the non-sun-synchronous orbit and the 74° inclination angle, CaSSIS is able to image sites at different

local times of different seasons, making CaSSIS images an ideal dataset for studying Martian surface changes. Up until 28 August 2021, CaSSIS images covered $\approx 4.3\%$ of the Martian surface.

In this work, we experiment with the TGO CaSSIS PAN band images over the Rosalind Franklin ExoMars rover's landing site at Oxia Planum. Up until 28 August 2021, CaSSIS has 100% coverage for the 1-sigma landing ellipses, about 92% coverage for the 3-sigma landing ellipses, and about 67% for the ExoMars RSOWG team's geological characterisation area of the landing site. Table 1 provides a list of the test CaSSIS images (selected for non-repeat), available overlapping HiRISE PDS DTMs and ORIs that are used for comparison/evaluation in (*Tao et al., 2021c*). It should be noted that both of the HiRISE PDS DTMs and the resultant CaSSIS MADNet DTM and CaSSIS SRR MADNet DTM mosaics have been 3D co-aligned with respect to the cascaded 12 m/pixel CTX and 25 m/pixel HRSC MADNet DTM mosaics (*Tao et al., 2021d*) that are both available on this ESA-PSA GSF, which themselves are co-aligned with the United States Geological Survey (USGS) MOLA areoid DTM v.2 (see https://astrogeology.usgs.gov/search/details/Mars/GlobalSurveyor/MOLA/Mars_MGS_MOLA_DEM_mosaic_global_463m/cub). Figure 1 shows an overview map of the test CaSSIS images (co-registered with the CTX and HRSC ORIs) superimposed on the CTX MADNet DTM mosaic.

Table 1. List of the input CaSSIS images (in the order of the image co-registration process – reverse order of the image and DTM mosaicing process), validation HiRISE PDS DTMs, and the corresponding HiRISE PDS ORIs, over the 3-sigma ellipses of the ExoMars Rosalind Franklin rover's landing site at Oxia Planum.

Input CaSSIS image ID	Overlapping HiRISE PDS DTM ID	HiRISE PDS ORI ID
MY35_007250_019_0	-	-
MY35_007623_019_0	-	-
MY35_008742_019_0 (cropped)	-	-
MY34_003806_019_2	DTEEC_039299_1985_047501_1985_L01	ESP_039299_1985_RED_A_01_ORTHO
MY34_004925_019_2	DTEEC_036925_1985_037558_1985_L01	ESP_036925_1985_RED_A_01_ORTHO
MY35_009481_165_0 (cropped)	-	-
MY35_013584_163_0 (cropped)	DTEEC_042134_1985_053962_1985_L01	ESP_042134_1985_RED_A_01_ORTHO
MY34_005664_163_2	-	-
MY34_005012_018_2	DTEEC_037070_1985_037136_1985_L01	ESP_037070_1985_RED_A_01_ORTHO

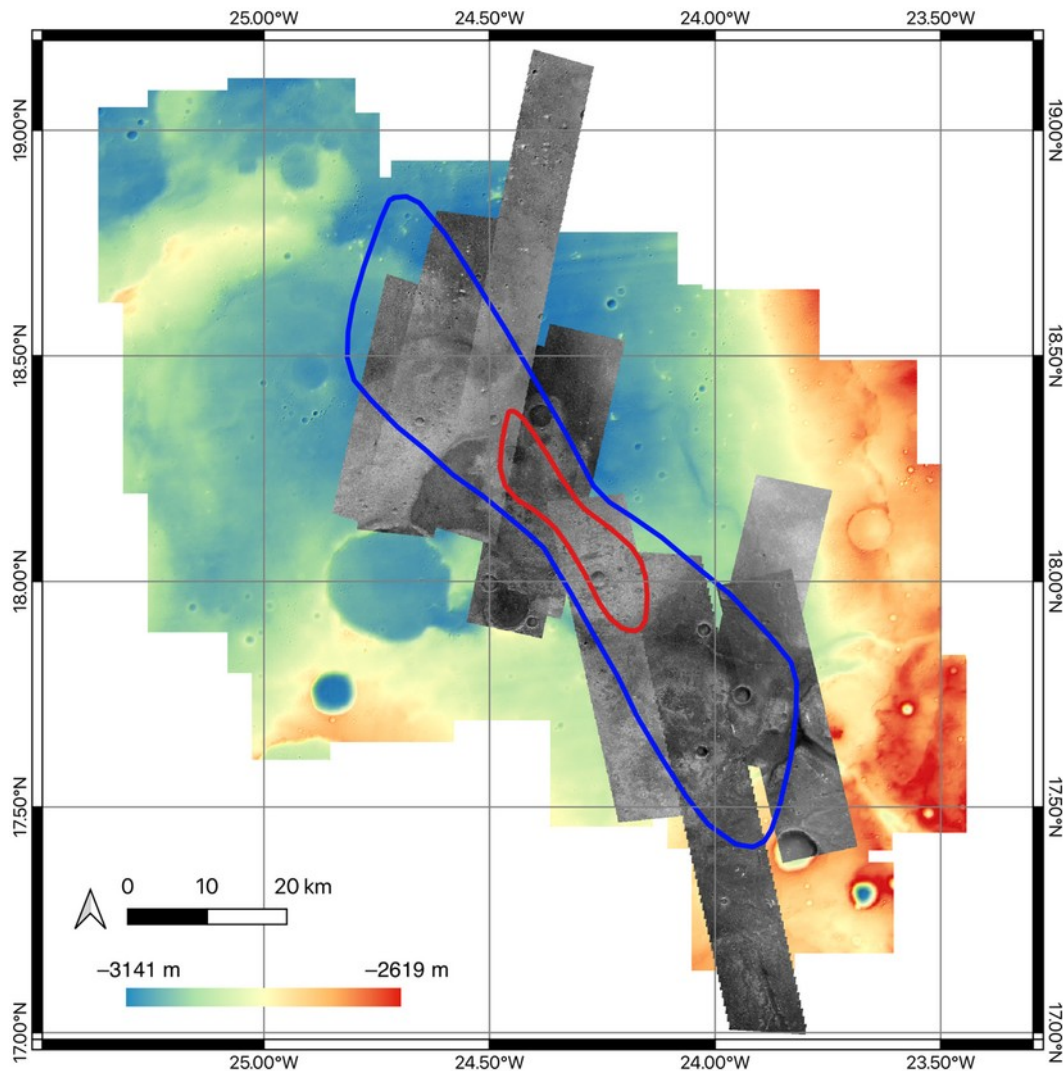


Figure 1. Overview map of the 9 test CaSSIS images (co-registered with the CTX and HRSC ORIs), superimposed on the CTX MADNet DTM mosaic (baseline reference), over the ExoMars Rosalind Franklin rover's landing site (1-sigma ellipse: red; 3-sigma ellipse: blue) at Oxia Planum (centred at 18.239°N, 24.368°W).

1.2 Abbreviations and Acronyms

DTM	Digital Terrain Model
DUG	Data User Guide
ESA	European Space Agency
GIS	Geographic Information System
TGO	Trace Gas Orbiter
CaSSIS	Colour and Stereo Surface Imaging System
HRSC	High-Resolution Stereo Camera
CTX	Context camera
HiRISE	High Resolution Imaging Science Experiments
MOLA	Mars Orbiter Laser Altimeter
NASA	National Aeronautics and Space Administration (United States)
ORI	OrthoRectified Images
PSA	Planetary Science Archive
UCL	University College London

1.3 Reference and Applicable Documents

Tao, Y.; Conway, S.J.; Muller, J.-P.; Putri, A.R.D.; Thomas, N.; Cremonese, G. Single Image Super-Resolution Restoration of TGO CaSSIS Colour Images: Demonstration with Perseverance Rover Landing Site and Mars Science Targets. *Remote Sens.* **2021**, *13*, 1777. <https://doi.org/10.3390/rs13091777>

Tao, Y.; Muller, J.-P.; Xiong, S.; Conway, S.J. MADNet 2.0: Pixel-Scale Topography Retrieval from Single-View Orbital Imagery of Mars Using Deep Learning. *Remote Sens.* **2021b**, *13*, 4220. <https://doi.org/10.3390/rs13214220>

Tao, Y.; Xiong, S.-T.; Muller, J.-P.; Michael, G.; Conway, S.J.; Paar, G.; Thomas, N.; Cremonese, G. Subpixel-Scale Topography Retrieval of Mars Using Single-Image DTM Estimation and Super-Resolution Restoration. *Remote Sensing* **2021c**, *in review*.

Tao, Y.; Muller, J.-P.; Conway, S.J.; Xiong, S. Large Area High-Resolution 3D Mapping of Oxia Planum: The Landing Site for the ExoMars Rosalind Franklin Rover. *Remote Sens.* **2021d**, *13*, 3270. <https://doi.org/10.3390/rs13163270>

2. SCIENTIFIC OBJECTIVES

All results shown here are made for the Rosalind Franklin ExoMars 2022 rover's landing site at Oxia Planum. This site is a 200 km wide clay bearing plain centred on 18.239°N, 24.368°W inside the United States Geological Survey (USGS)'s Oxia Palus (MC-11) quadrangle of Mars. The landing site area straddles the dichotomy boundary of Mars, which separates the northern lowlands from the southern highlands. The site slopes towards the north and hosts mineralogical (iron-magnesium rich clay minerals) and geomorphological evidence of liquid water in the ancient past, which motivated the choice of this site for this mission whose principal objective is to search for potential biomarkers indicating past life on Mars.

2.1 Acknowledgements

Users are requested to acknowledge the dataset by mentioning it in any relevant figure captions and within acknowledgement within their publications to cite both the DOI of the dataset and the paper describing the processing system, assessment, and mosaic generation:

Tao, Y.; Conway, S.J.; Muller, J.-P.; Putri, A.R.D.; Thomas, N.; Cremonese, G. Single Image Super-Resolution Restoration of TGO CaSSIS Colour Images: Demonstration with Perseverance Rover Landing Site and Mars Science Targets. *Remote Sens.* **2021**, *13*, 1777. <https://doi.org/10.3390/rs13091777>

Tao, Y.; Muller, J.-P.; Xiong, S.; Conway, S.J. MADNet 2.0: Pixel-Scale Topography Retrieval from Single-View Orbital Imagery of Mars Using Deep Learning. *Remote Sens.* **2021b**, *13*, 4220. <https://doi.org/10.3390/rs13214220>

Tao, Y.; Xiong, S.-T.; Muller, J.-P.; Michael, G.; Conway, S.J.; Paar, G.; Thomas, N.; Cremonese, G. Subpixel-Scale Topography Retrieval of Mars Using Single-Image DTM Estimation and Super-Resolution Restoration. *Remote Sensing* **2021c**, *in review*.

Tao, Y.; Muller, J.-P.; Conway, S.J.; Xiong, S. Large Area High-Resolution 3D Mapping of Oxia Planum: The Landing Site for the ExoMars Rosalind Franklin Rover. *Remote Sens.* **2021d**, *13*, 3270. <https://doi.org/10.3390/rs13163270>

The research leading to these results receiving funding from the UKSA Aurora programme (2018–2021) under grant ST/S001891/1, as well as partial funding from the STFC MSSL Consolidated Grant ST/K000977/1.

3. DATA PRODUCT GENERATION

The processing core of this work is the deep learning based MARSGAN SRR and MADNet SDE systems described in (*Tao et al., RS, 2021a-c*). MARSGAN and MADNet are based on the relativistic GAN framework that involves training of a generator network and a discriminator network in parallel. For the MARSGAN SRR, the generator network is trained to produce potential SRR estimates, whilst the discriminator network is trained in parallel (and updated in an alternating manner with the generator network) to estimate the probability of the given training HR images being more realistic than the generated SRR images on average. Whereas for MADNet SDE, the generator network is trained to produce per pixel relative heights, and the discriminator network is trained to distinguish the predicted heights from the ground-truth heights.

For the MARSGAN generator network, we employ a feed-forward residual convolutional neural network (CNN) architecture, consisting of twenty-three Adaptive Weighted Residual-in-Residual Dense Blocks (AWRRDBs), followed by an Adaptive Weighted Multi-Scale Reconstruction (AWMSR) block. Each of the AWRRDBs contains eleven independent weights, three DCBs, and additive noise inputs on top of the residual-in-residual structure. For the MADNet generator network, we employ a fully convolutional U-net architecture, consisting of four stacks of DCBs as the encoder and five stacks of Up-Projection Blocks (UPBs) as the decoder. MARSGAN and MADNet use a similar discriminator network architecture as detailed in (*Tao et al., RS, 2021a, 2021b*). Simplified network architectures of the MARSGAN SRR and MADNet SDE networks that are used in this work are shown in Figure 2.

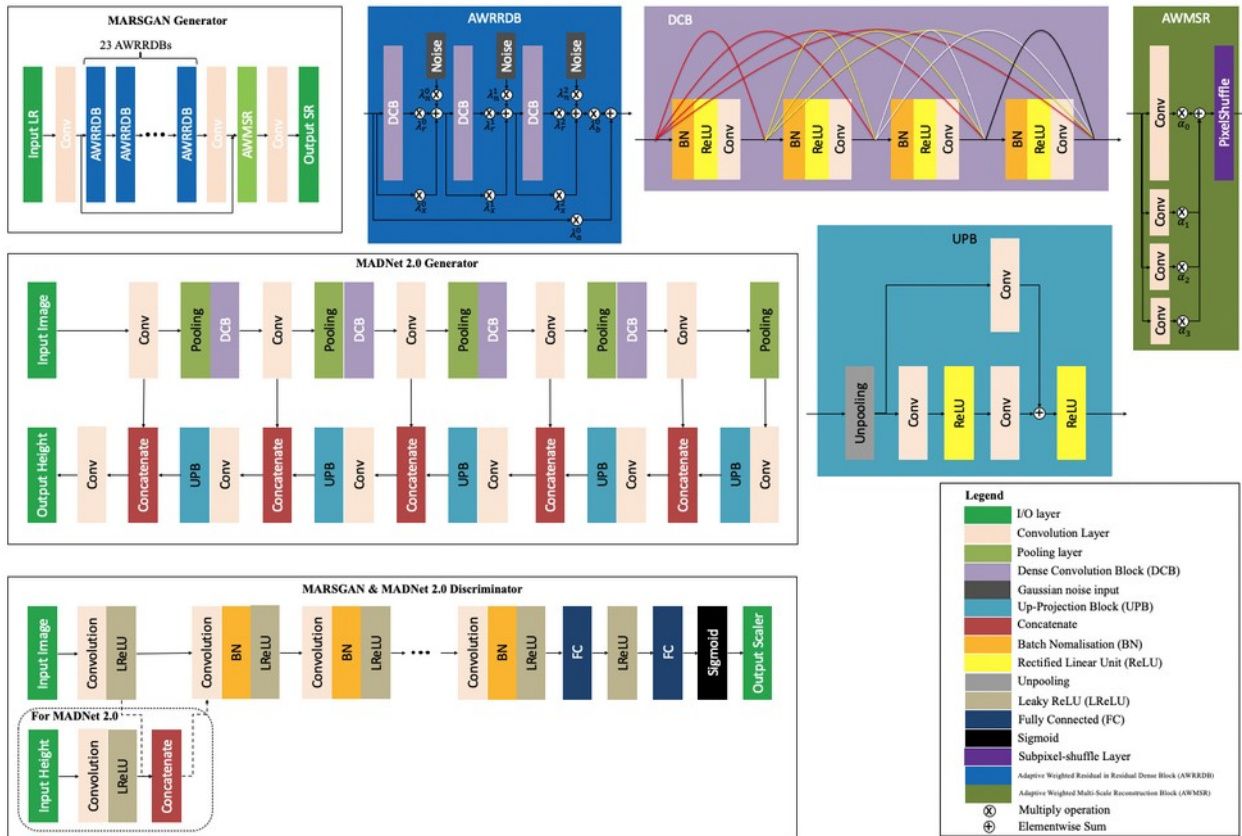


Figure 2. Network architectures of MARSGAN and MADNet.

Archive Format and Content

3.1 Product Overview

A variety of novel products have been generated including nine single-strip CaSSIS PAN band 1 m/pixel SRR images and 2 m/pixel SRR-DTMs, a brightness and contrast corrected 1 m/pixel CaSSIS SRR greyscale image mosaic, a 1 m/pixel CaSSIS SRR colour image mosaic (coloured using HRSC colour by G. Michael of the Free University Berlin, due to the CaSSIS colour bands being much narrower than the PAN band), an 8 m/pixel CaSSIS DTM mosaic, and a 2 m/pixel CaSSIS SRR-DTM mosaic, over the 3-sigma ellipses of the ExoMars Rosalind Franklin rover’s planned landing site at Oxia Planum. Figure 3 shows overview maps of the original 4 m/pixel CaSSIS NPB (NIR-PAN-BLU) band colour images, the resultant 1 m/pixel CaSSIS PAN band SRR single-strip images, 1 m/pixel CaSSIS SRR image mosaic, 1 m/pixel CaSSIS SRR image mosaic with HRSC colour, 8 m/pixel CaSSIS MADNet DTM mosaic and shaded relief image (330° azimuth, 30° altitude, 2× vertical exaggeration), and the 2 m/pixel CaSSIS SRR MADNet DTM mosaic and shaded relief image (330° azimuth, 30° altitude, 2× vertical exaggeration). It should be noted that all CaSSIS SRR, MADNet DTM, and SRR MADNet DTM results are produced using the 4 m/pixel CaSSIS PAN band images, the 4 m/pixel CaSSIS NPB colour images that are shown in Figure 3 are for information only to show their narrower coverage and the reason why they are not used in this work (gaps between the adjacent colour images).

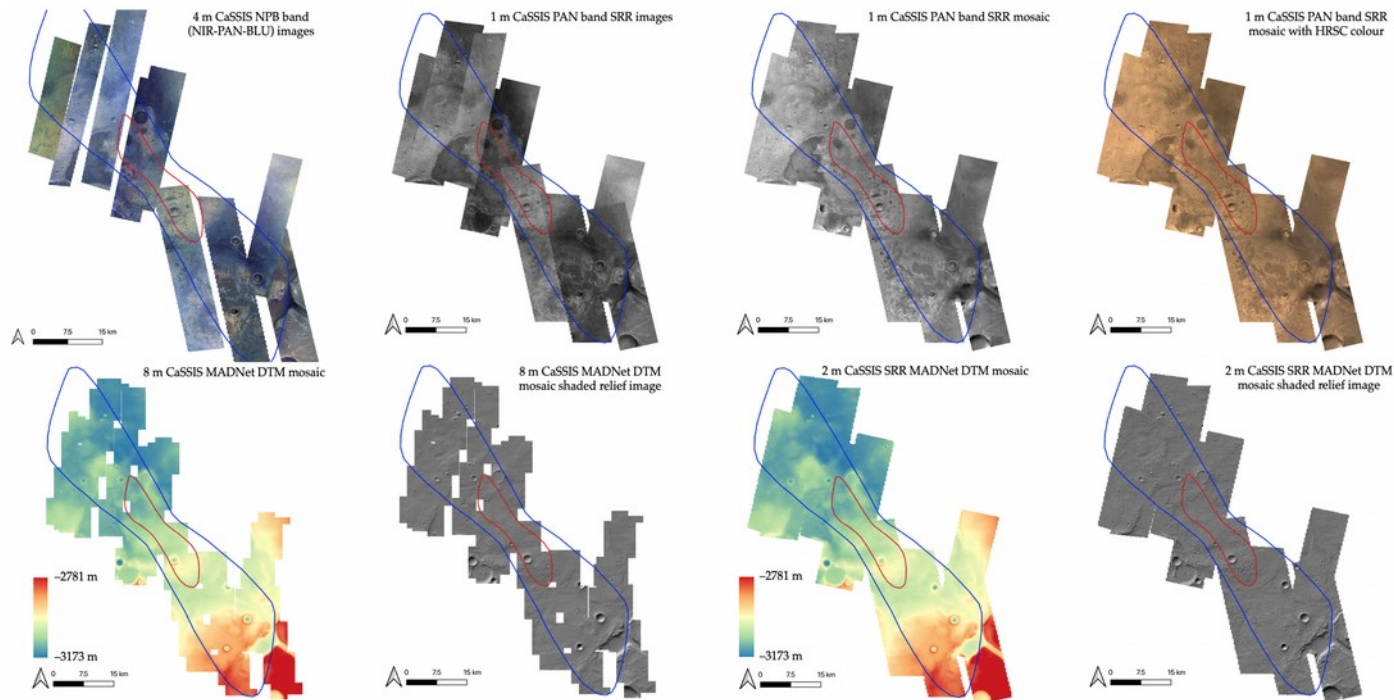


Figure 3. Overview maps of the 4 m/pixel CaSSIS NPB (NIR-PAN-BLU) band colour images, the resultant 1 m/pixel CaSSIS PAN band SRR single-strip images, 1 m/pixel CaSSIS SRR image mosaic, 1 m/pixel CaSSIS SRR image mosaic with HRSC colour, 8 m/pixel CaSSIS MADNet DTM mosaic, shaded relief image of the 8 m/pixel CaSSIS MADNet DTM mosaic, 2 m/pixel CaSSIS SRR MADNet DTM mosaic, and shaded relief image of the 2 m/pixel CaSSIS SRR MADNet DTM mosaic, over the 1-sigma (red) and 3-sigma (blue) ellipses of the ExoMars Rosalind Franklin rover's planned landing site at Oxia Planum.

The above results (SRR image and SRR-DTM) at a very high resolution with uniform quality and consistency are being published through the ESA GSF. They are spatially co-registered and vertically co-aligned with respect to the cascaded HiRISE, CTX, and HRSC ORIs and DTM mosaics that are described in (*Tao et al., RS, 2021c, 2021d*), which themselves are accurately co-registered with the ESA/DLR/FUB HRSC MC-11W level 5 ORI mosaic (available at <http://hrscteam.dlr.de/HMC30>) and vertically co-aligned with the aforementioned USGS MOLA areoid DTM. We use identical map projection system (Equidistant Cylindrical) and map projection parameters as used in the ESA/DLR/FUB HRSC MC-11W level 5 ORI and DTM products. These other products are also available through the ESA-PSA GSF at

https://www.cosmos.esa.int/web/psa/ucl-mssl_oxia-planum_hrsc_ctx_hirise_madnet_1.0

3.2 SRR and SRR-DTM Product Specification

- Projection: Equirectangular (aka Equidistant Cylindrical) ¹
- Mars radius reference: MOLA aeroid (da) ²

Product	Filename	Image size (pixels)	Resolution (m/pixel)	Bit-depth
CaSSIS PAN band SRR image mosaic (greyscale)	cassis_pan_srr_mosaic.tif	69097 x 85710	1	Byte
CaSSIS SRR image mosaic (with HRSC colour)	cassis_pan_srr_mosaic_hrsc_rgb_colour.tif	69097 x 85710	1	Byte
CaSSIS MADNet DTM mosaic	CaSSIS-MADNet-DTM-mosaic-ORDERED.tif	8330 x 10428	8	Float32
CaSSIS SRR MADNet DTM mosaic	CaSSIS-SRR-MADNet-DTM-mosaicv2.tif	34197 x 42719	2	Float32

3.3 Product Example and Usage

The DTM and SRR image file are in GeoTiff format and can be opened by many different GIS/image processing systems such as ArcGIS, QGIS, and ENVI. Projection and mapping information is embedded in the tags of the Geotiff file. The best way to visually inspect a DTM is by using a coloured hill-shaded display. The following instructions show how to create a coloured hill-shaded view of the DTM product in QGIS.

1. Import the DTM via: Layer -> Add layer -> Add Raster Layer -> Select the Raster dataset(s) -> Add -> Close
2. Create shaded relief image: left click to select the DTM -> Raster -> Analysis -> Hillshade -> Select the illumination parameters (e.g., z=2, azimuth=330, elevation=30) under “Hillshade” click “...” -> save to file -> choose a filename and end with .tif -> OK -> run -> close
3. Adjust the display setting of the shaded relief image: right click the hill-shaded relief image -> Properties -> Symbology -> under “Color Rendering” select “Blending mode” -> “Overlay” -> adjust “Brightness” as “-60” -> Apply -> OK.
4. Adjust the display setting of the DTM: right click the DTM -> Properties -> Symbology -> under “Band Rendering” select “Render type” as “Singleband pseudocolor” -> under “Min/Max Value Settings” select Min/Max -> under “Color ramp” select a colour ramp then select “Invert Color Ramp” -> click “Classify” -> Apply -> OK

Other important points to note:

1. Ensure you place the hillshaded relief image layer in front of the coloured DTM layer.
2. Do not use transparency for the hillshaded relief image layer as “Overlay” display mode is already selected.
3. You can use z=3 if a strong hill-shading effect is required.

¹ https://en.wikipedia.org/wiki/Equirectangular_projection

² https://astrogeology.usgs.gov/search/map/Mars/GlobalSurveyor/MOLA/Mars_MGS_MOLA_DEM_mosaic_global_463m

4. Always create a group for the colourised DTM and hillshaded relief image and use the group icon to toggle display of the colourised hillshaded DTM.

4. KNOWN ISSUES

In this work, we have demonstrated that DTM production, at 2 times higher resolution than the original input image, is feasible from single-view Mars orbital images (i.e., CaSSIS) using deep learning based SRR and SDE methods. We observe significant improvements both qualitatively and quantitatively from the resultant MADNet DTMs that use MARSGAN SRR compared to the MADNet DTMs that do not use MARSGAN SRR. The improvement of DTM resolution is visually about 4 times but quantitatively better than 4 times, even though the improvement of the images themselves via MARSGAN SRR is visually and quantitatively less than 4 times (*Tao et al., RS, 2021c*). We believe that most of the improvement of the DTM resolution comes from the improved image resolution, and the “extra” improvement comes from the reduction of image noise which leads to better performance of the MADNet SDE process.

While the improvement in the DTM resolution is encouraging, the coupled SRR and SDE process slightly lowers the accuracy (RMSE difference 0.323 m) and structural similarity (SSIM difference 0.049) for the resultant CaSSIS DTM, which implies higher DTM uncertainty. This quantitative evaluation also agrees with our visual inspection that topographic features in the CaSSIS SRR MADNet DTM are subject to minor overshoot/undershoot or shape differences, compared to the HiRISE image and HiRISE SRR MADNet DTM, even though they look plausible when compared to the original CaSSIS and CaSSIS SRR image. This is due to the fact that MARSGAN SRR attempts to give the most realistic HR estimation of the fine-scale features but cannot “invent” the HR features or textures that are not visible from the input image. Such HR estimation is based on the existing information in the input image that is partially subject to interference from sensor/atmosphere noise and/or incompletely recorded pixel-scale information, which could consequently give inaccurate or erroneous SRR input to the follow-up MADNet SDE process.

Figure 4 shows input images and shaded relief images of the output DTMs of an exemplar area over a subarea (south-west corner) of a small crater (centred at 24.3350°W, 18.0716°N) of the test site at Oxia Planum. The “red arrows” show an example of the CaSSIS features that are considered inaccurately super-resolved, where the “real” feature appears to be wider in the 25 cm/pixel HiRISE image, compared to the narrower appearance in the 1 m/pixel CaSSIS SRR image, and consequently, such features are inaccurately interpreted in 3D, where the “real” feature appears to be flatter and thicker in the 50 cm/pixel HiRISE MADNet DTM, compared to their steeper and thinner appearance in the 2 m/pixel CaSSIS SRR MADNet DTM. The “green arrows” show a counter example of the same features that are considered more accurately super-resolved, where the “real” feature appears to have a very similar width and shape in the HiRISE image and CaSSIS SRR image, and subsequently, results in a fairly similar appearance of its 3D shape and slope in the shaded relief images of the HiRISE MADNet DTM and CaSSIS SRR MADNet DTM. This example demonstrates the resultant CaSSIS SRR MADNet DTM contains a mixture of reliable topography as well as less accurate topography, though with obviously higher effective resolution.

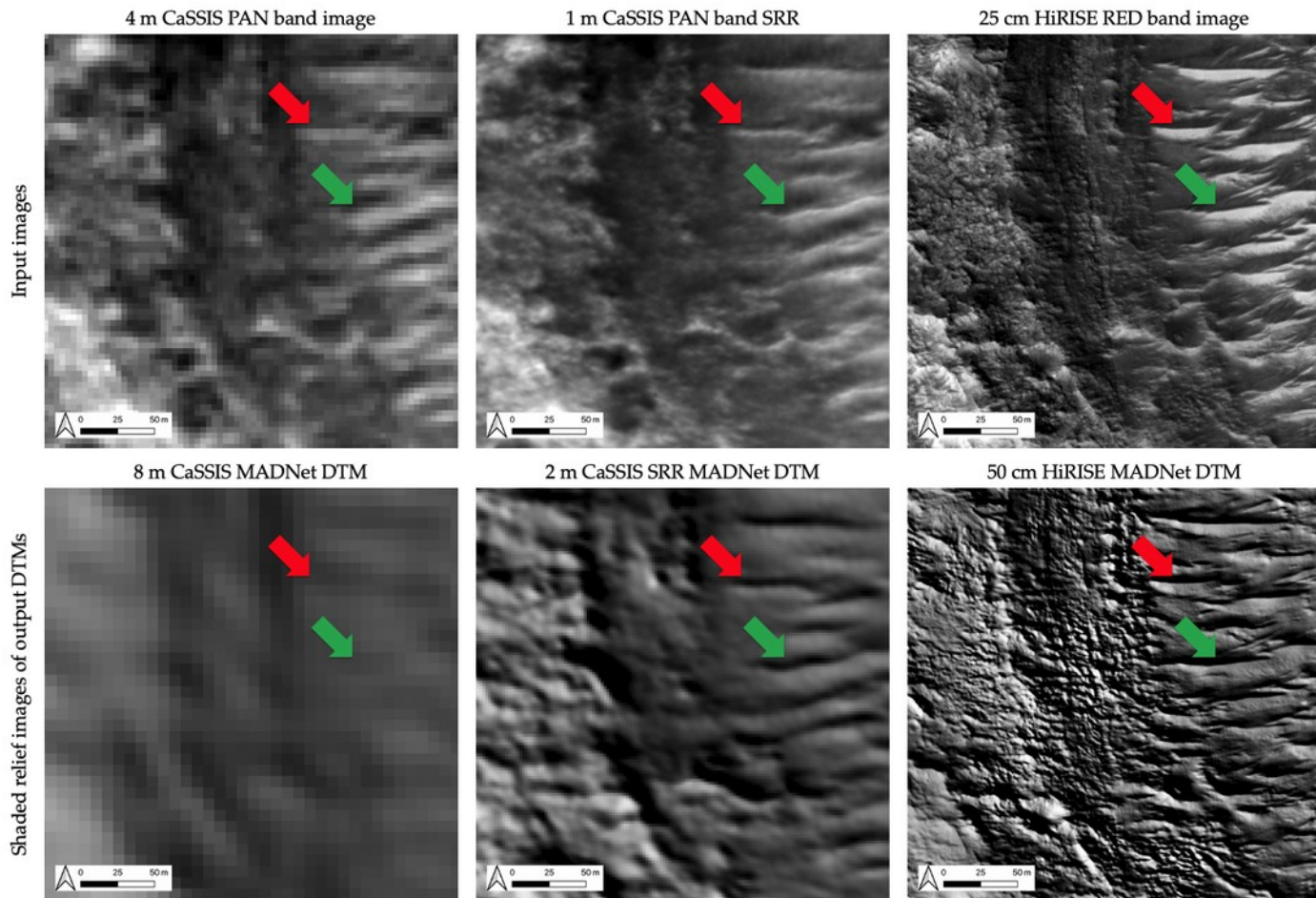


Figure 4. Images and shaded relief images of the corresponding DTM products showing a portion (south-west corner) of a small crater (centred at 24.3350°W , 18.0716°N) of the test site at Oxia Planum. 1st row: 4 m/pixel CaSSIS PAN band image (MY35_009481_165_0_PAN), 1 m/pixel CaSSIS PAN band SRR image, and 25 cm/pixel HiRISE RED band PDS ORI (ESP_039299_1985_RED_A_01_ORTHO); 2nd row: shaded relief images (using similar illumination parameters as the HiRISE PDS ORI, i.e., 225° azimuth, 30° altitude, $2\times$ vertical exaggeration) of the 8 m/pixel CaSSIS MADNet DTM, 2 m/pixel CaSSIS SRR MADNet DTM, and 50 cm/pixel HiRISE MADNet DTM. Red arrows point to an exemplar of the super-resolved features and their topography that are considered less accurate compared to the HiRISE images and DTMs. Green arrows point to an exemplar of the super-resolved features and their topography that are considered more accurate compared to the HiRISE images and DTMs.

5. SOFTWARE

The processing uses the UCL's in-house MARSGAN SRR and MADNet SDE software.